High-Order Finite-Volume Methods for Hyperbolic Problems

Phillip Colella
Computational Research Division
Lawrence Berkeley National Laboratory

Why Higher Order ?

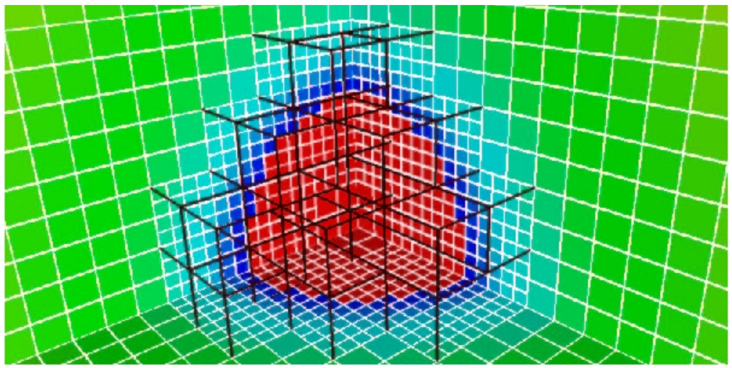

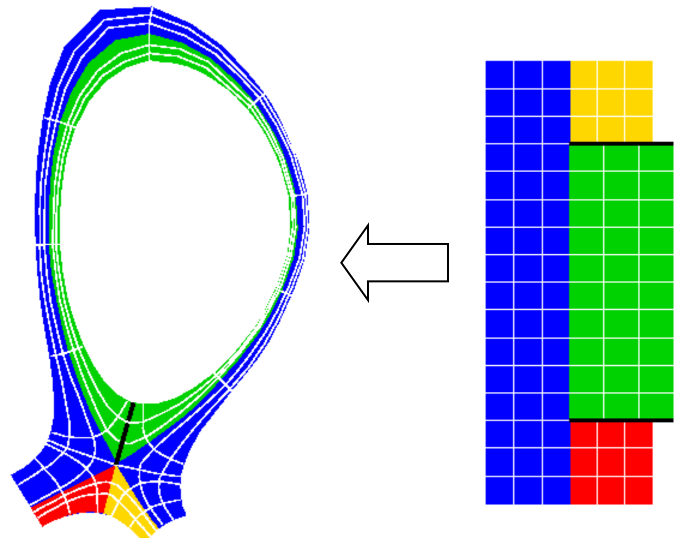

- Locally-refined grids, mapped-multiblock grids – smooth except at boundaries between different refinement levels / blocks. Leads to loss of one order of accuracy at boundaries: $2^{nd} \rightarrow 1^{st}$, $4^{th} \rightarrow 3^{rd}$.
- Over the next decade, bytes / flop expected to go down by 10x. Similar relative increases in imbalance between communication and computation (higher latencies, lower bandwidth). Want to do more computation per unit of data access, use less data overall.

Finite-Volume Methods on Structured Grids

We use the divergence theorem for computing the average of div(F) over a control volume.

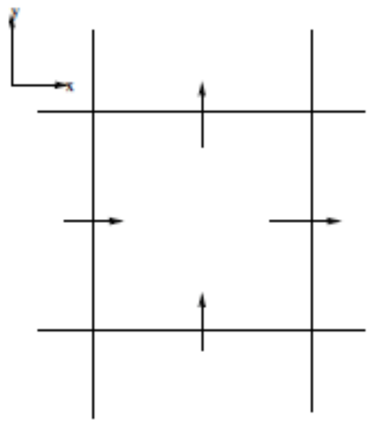

$$-\frac{1}{h^D}\int_{V_{\boldsymbol{i}}} \nabla \cdot \vec{F} d\boldsymbol{x} = -\frac{1}{h}\sum_d \langle F^d \rangle_{\boldsymbol{i}+\frac{1}{2}\boldsymbol{e}^d} - \langle F^d \rangle_{\boldsymbol{i}-\frac{1}{2}\boldsymbol{e}^d}$$

$$\langle F^d \rangle_{\boldsymbol{i}+\frac{1}{2}\boldsymbol{e}^d} \equiv \frac{1}{h^{D-1}}\int_{A_d^{\pm}} F^d(\boldsymbol{x},t)dA$$

• This is an exact relationship – the approximations are introduced by the choice of quadrature for the face integrals.
• For smooth grids, the truncation error of the approximation to the average of div(F) is the same as the truncation the error in the flux (standard centered-difference error cancellation applies here as well).

Design Issues for High-Order Finite-Volume Methods

- High-order quadratures for fluxes.
- Limiters for hyperbolic problems.
- Time-dependent problems: time discretizations, semi-implicit methods.
- Adaptive mesh refinement.
- Extension to mapped grids, multiblock grids.

High-Order Quadratures for Fluxes

At second-order accuracy, can approximate averages by the midpoint rule. For higher-order accuracy, must distinguish between cell averages, face averages, and point values.

$$\langle F^d \rangle_{\boldsymbol{i} \pm \frac{1}{2}\boldsymbol{e}^d} = \frac{1}{h^{D-1}} \int\limits_{A_d^{\pm}} F^d dA,$$

$$\langle F^d \rangle = F^d(\boldsymbol{x}_0) + \frac{h^2}{24} \sum_{d' \neq d} \frac{\partial^2 F_d}{\partial x_{d'}^2} + O(h^4)$$

$$\langle fg \rangle_{\boldsymbol{i}} = \langle f \rangle_{\boldsymbol{i}} \langle g \rangle_{\boldsymbol{i}} + \frac{h^2}{12} \nabla f \cdot \nabla g + O(h^4)$$

$$\langle fg \rangle_{\boldsymbol{i}+\frac{1}{2}\boldsymbol{e}^d} = \langle f \rangle_{\boldsymbol{i}+\frac{1}{2}\boldsymbol{e}^d} \langle g \rangle_{\boldsymbol{i}+\frac{1}{2}\boldsymbol{e}^d} + \frac{h^2}{12} \sum_{d' \neq d} \frac{\partial f}{\partial x_{d'}} \frac{\partial g}{\partial x_{d'}} + O(h^4)$$

These can be used to compute more general nonlinear functions:

$$\langle W(U) \rangle = W(\langle U \rangle) + O(h^2)$$

$$U_{\boldsymbol{i}} = \langle U \rangle_{\boldsymbol{i}} - \frac{h^2}{24} \Delta^{(2)} \langle U \rangle_{\boldsymbol{i}} \qquad W_{\boldsymbol{i}} = W(U_{\boldsymbol{i}}) \qquad \langle W \rangle_{\boldsymbol{i}} = W_{\boldsymbol{i}} + \frac{h^2}{24} \Delta^{(2)} \overline{W}_{\boldsymbol{i}} \qquad \overline{W}_{\boldsymbol{i}} = W(\langle U \rangle_{\boldsymbol{i}})$$

"Convolution / deconvolution"

Ref: Barad and Colella, 2005

Semi-Discrete Formulation of Finite-Volume Methods for Time-Dependent Problems

We can integrate conservation laws

$$\frac{\partial U}{\partial t} + \nabla \cdot \vec{F} = 0$$

over rectangular control volumes

$$V_{\boldsymbol{i}} = [\boldsymbol{i}h, (\boldsymbol{i}+\boldsymbol{u})h] \ , \ \boldsymbol{i} \in \mathbb{Z}^D \ , \ \boldsymbol{u} = (1, 1, \dots, 1)$$

to obtain a system of ordinary differential equations

$$\frac{d\langle U \rangle_{\boldsymbol{i}}}{dt} = -\frac{1}{h^D} \int\limits_{V_{\boldsymbol{i}}} \nabla \cdot \vec{F} d\boldsymbol{x} = -\frac{1}{h} \sum_d \langle F^d \rangle_{\boldsymbol{i}+\frac{1}{2}\boldsymbol{e}^d} - \langle F^d \rangle_{\boldsymbol{i}-\frac{1}{2}\boldsymbol{e}^d}$$

$$\langle U \rangle_{\boldsymbol{i}} \equiv -\frac{1}{h^D} \int\limits_{V_{\boldsymbol{i}}} U(\boldsymbol{x}, t) d\boldsymbol{x} \qquad \langle F^d \rangle_{\boldsymbol{i}+\frac{1}{2}\boldsymbol{e}^d} \equiv \frac{1}{h^{D-1}} \int\limits_{A_d^{\pm}} F^d(\boldsymbol{x}, t) dA$$

We use a method of lines approach, separating spatial and temporal discretization.

Active Development for Applications

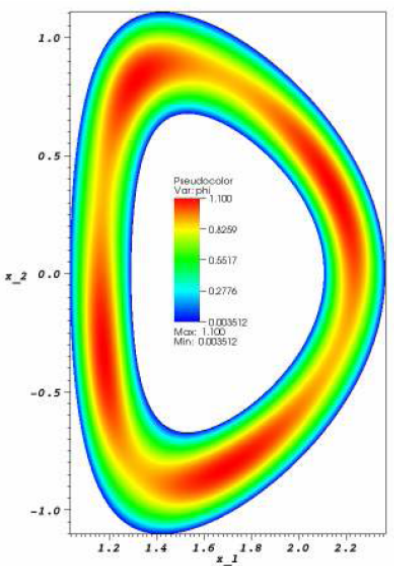

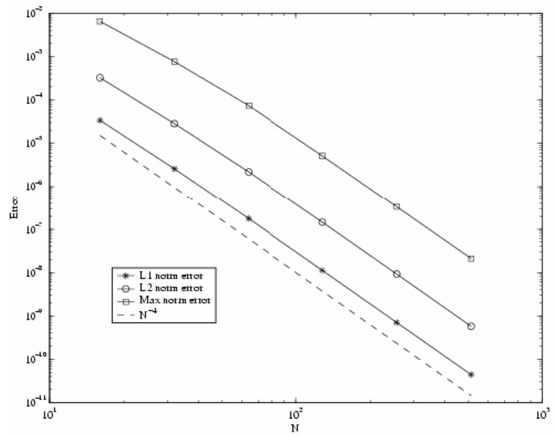

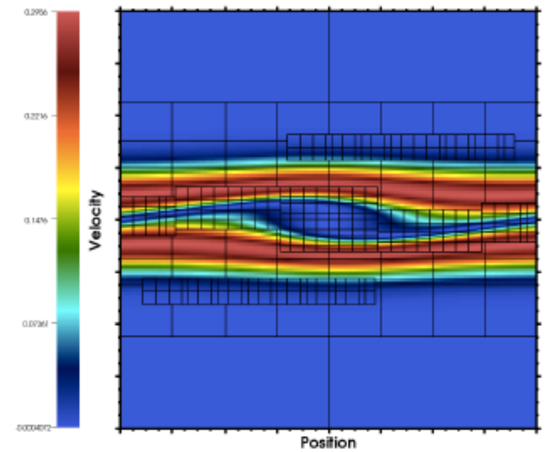

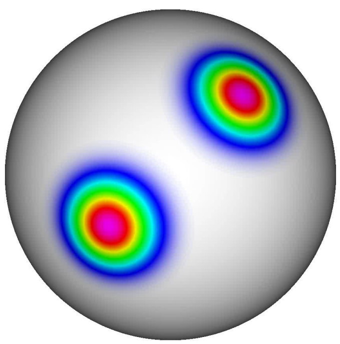

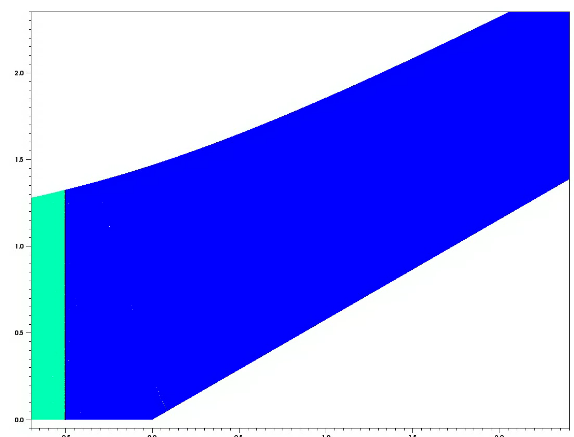

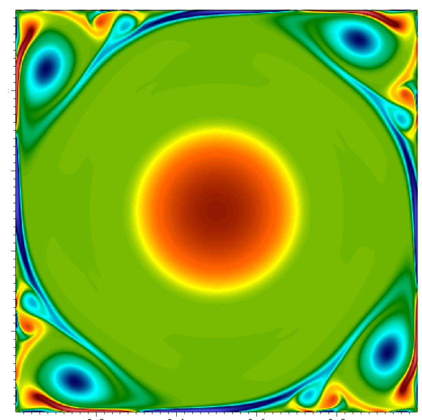

BERKELEY LAB
LAWRENCE BERKELEY NATIONAL LABORATORY

U.S. DEPARTMENT OF ENERGY
Office of Science

Runge-Kutta Time Integration

$$\frac{d\langle U \rangle}{dt} = -D \cdot \vec{F};$$

$$D \cdot \vec{F} = D \cdot \vec{F}(\langle U \rangle) = \frac{1}{h} \sum_d \langle F^d \rangle_{\boldsymbol{i}+\frac{1}{2}\boldsymbol{e}^d} - \langle F^d \rangle_{\boldsymbol{i}-\frac{1}{2}\boldsymbol{e}^d}.$$

Then, starting with $\langle U \rangle^{(0)} = \langle U \rangle(t^n)$, set

$$k_1 = -D \cdot \vec{F}(\langle U \rangle^{(0)})\Delta t;$$

$$\langle U \rangle^{(1)} = \langle U \rangle^{(0)} + \frac{k_1}{2}; \qquad k_2 = -D \cdot \vec{F}(\langle U \rangle^{(1)})\Delta t;$$

$$\langle U \rangle^{(2)} = \langle U \rangle^{(0)} + \frac{k_2}{2}; \qquad k_3 = -D \cdot \vec{F}(\langle U \rangle^{(2)})\Delta t;$$

$$\langle U \rangle^{(3)} = \langle U \rangle^{(0)} + k_3; \qquad k_4 = -D \cdot \vec{F}(\langle U \rangle^{(3)})\Delta t.$$

Then to integrate one time step:

$$\langle U \rangle(t^n + \Delta t) = \langle U \rangle(t^n) + \frac{1}{6}(k_1 + 2k_2 + 2k_3 + k_4) + O((\Delta t)^5).$$

This update can be written as the difference of a sum of fluxes:

$$F^H_{\boldsymbol{i}+\frac{1}{2}\boldsymbol{e}^d} = \frac{1}{6}(F^{(0)} + 2F^{(1)} + 2F^{(2)} + F^{(3)})_{\boldsymbol{i}+\frac{1}{2}\boldsymbol{e}^d}$$

Extremum-Preserving Limiters

Commonly used approach: geometric limiting applied at each stage of RK. At extrema, compare different estimates of second derivatives to determine degree of limiting.

Issues:

• Geometric limiting at each stage -> time step limited by donor cell, scales like 1/(Dimension).

• Centered differencing is dissipation-free, interaction with RK + stage-wise limiters is brittle.

• Alternative approach:

  – Use upstream-centered differencing for high-order method.

  –Apply 1979 Zalesak extremum-preserving FCT to the sum of the fluxes at the end of the time step; leaves us free to choose low-order method (e.g. corner-coupled upwind methods).

  – Compute bounds on extrema using local quadratic interpolation.

FCT Limiters (Zalesak, 1979)

$$A_{i+(1/2)} \equiv F^H_{i+(1/2)} - F^L_{i+(1/2)}$$

$$w_i^{td} = w_i^{\ n} - \Delta x_i^{-1}[F^L_{i+(1/2)} - F^L_{i-(1/2)}]$$

$$w_i^{n+1} = w_i^{td} - \Delta x_i^{-1}[A^C_{i+(1/2)} - A^C_{i-(1/2)}]$$

$$A^C_{i+(1/2)} = C_{i+(1/2)} A_{i+(1/2)}\,, \qquad 0 \leqslant C_{i+(1/2)} \leqslant 1$$

FCT Limiters (Zalesak, 1979)

$$P_i^+ = \text{the sum of all antidiffusive fluxes } \textit{into} \text{ grid point } i$$

$$= \max(0, A_{i-(1/2)}) - \min(0, A_{i+(1/2)})$$

$$Q_i^+ = (w_i^{\max} - w_i^{td})\,\Delta x_i$$

$$R_i^+ = \begin{Bmatrix} \min(1, Q_i^+/P_i^+) & \text{if} \quad P_i^+ > 0 \\ 0 & \text{if} \quad P_i^+ = 0 \end{Bmatrix}$$

$$P_i^- = \text{the sum of all antidiffusive fluxes } \textit{away from} \text{ grid point } i$$

$$= \max(0, A_{i+(1/2)}) - \min(0, A_{i-(1/2)})$$

$$Q_i^- = (w_i^{td} - w_i^{\min})\,\Delta x_i$$

$$R_i^- = \begin{Bmatrix} \min(1, Q_i^-/P_i^-) & \text{if} \quad P_i^- > 0 \\ 0 & \text{if} \quad P_i^- = 0 \end{Bmatrix}$$

$$C_{i+(1/2)} = \begin{cases} \min(R_{i+1}^+, R_i^-) & \text{if} \quad A_{i+(1/2)} \geqslant 0 \\ \min(R_i^+, R_{i+1}^-) & \text{if} \quad A_{i+(1/2)} < 0 \end{cases}$$

FCT Limiters (Zalesak, 1979)

Strategy: at smooth extrema, compute bounds on solution that cause the limiter to switch off.

1. How does one detect a smooth extremum ?
2. How does one compute bounds at such an extremum?

Answer to (1): Look for change in sign of derivative, then measure the relative size of the local total variation of the solution and the difference between the two endpoints:

$$|\rho_{i+2} - \rho_{i-2}| \leq K \sum_{s=-1}^{2} |\rho_{i+s} - \rho_{i+s-1}|$$

At a smooth quadratic extremum, K = 2 + O(h). If the above is true for some K ~1.25-1.5 and the sign of the first derivative changes, we assume to be at a smooth extremum.

Answer to (2): look at the max or min of interpolated quadratics at the cell and on the cells to the left and right, then scale the extremum defined by them by a constant factor (we use 2). Analogous to van Leer limiting in monotone regions.

Upstream-Centered Differencing

$$\frac{\partial \rho}{\partial t} + \frac{\partial \rho}{\partial x} = 0$$

$$\rho_{j+\frac{1}{2}} = \frac{1}{60}(\rho_{j-2} - 8\rho_{j-1} + 37\rho_j + 37\rho_{j+1} - 8\rho_{j+2} + \rho_{j+3}) \text{ (Centered)}$$

$$= \frac{1}{60}(-\rho_{j-3} + 7\rho_{j-2} - 23\rho_{j-1} + 57\rho_j + 22\rho_{j+1} - 2\rho_{j+2}) \text{ (Upstream-Centered)}$$

Both are sixth-order accurate approximations to $\frac{\partial}{\partial x}\int^{x} \rho(x', t)dx'\Big|_{(j+\frac{1}{2})\Delta x}$

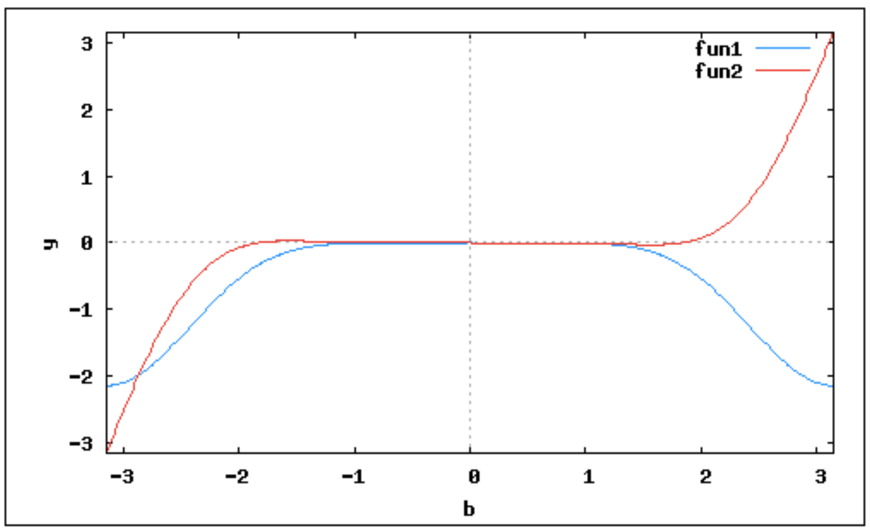

Von Neumann analysis of upstream-centered operator.
Red - imaginary part of the error.
Blue - real part of the error.

Example: Square Wave, CFL=.1

Centered | Upstream-centered

No limiter
(T = 1,N=256)

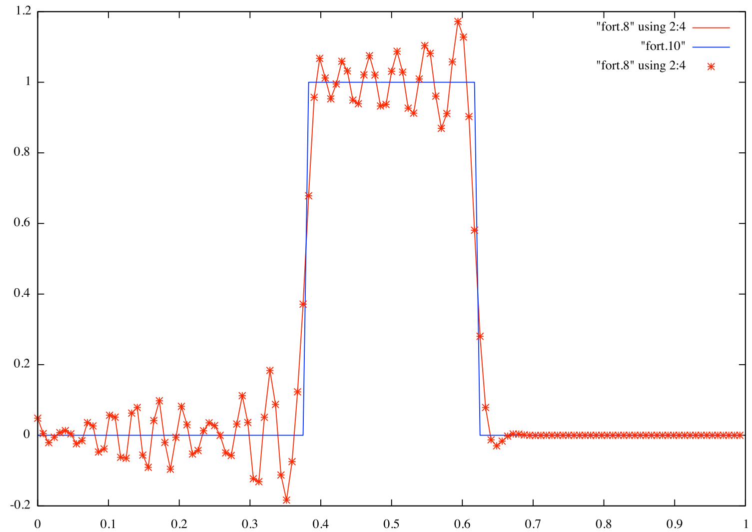

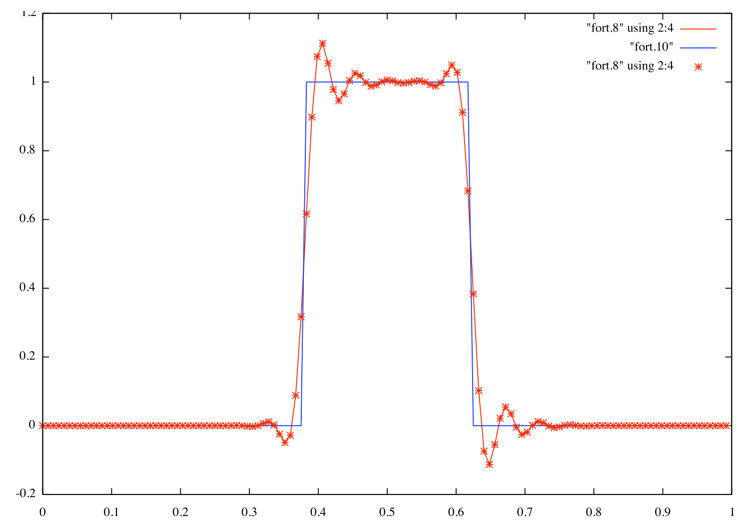

Limiter
(T = 10, N=128)

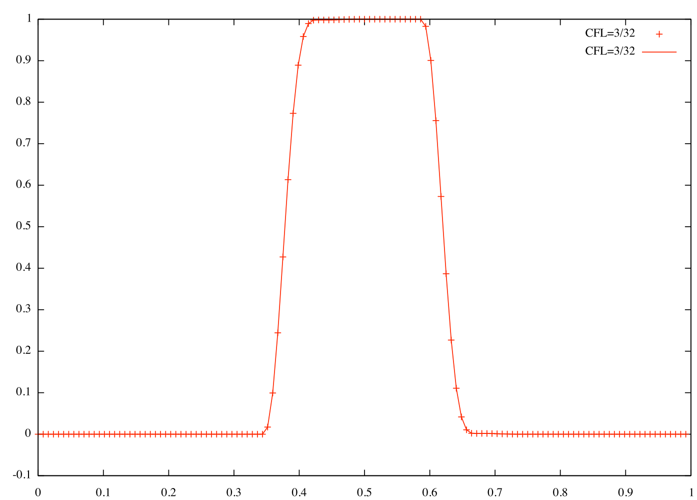

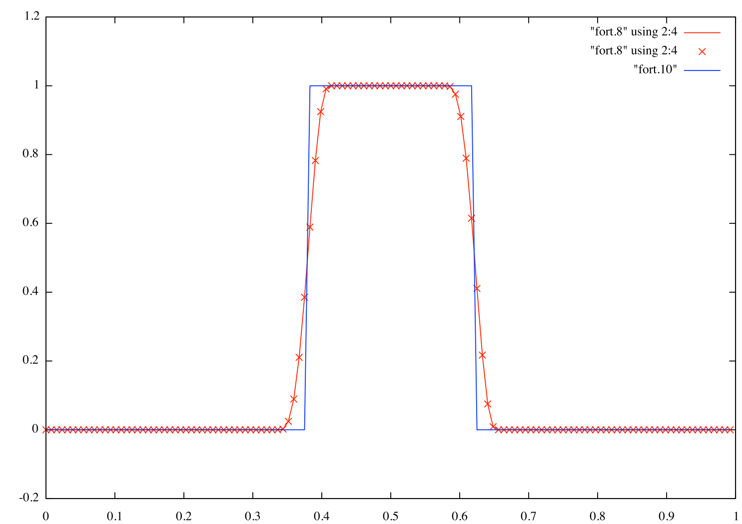

BERKELEY LAB
LAWRENCE BERKELEY NATIONAL LABORATORY

U.S. DEPARTMENT OF ENERGY | Office of Science

Example: Semicircle, CFL=.1

Centered | Upstream-centered

No limiter

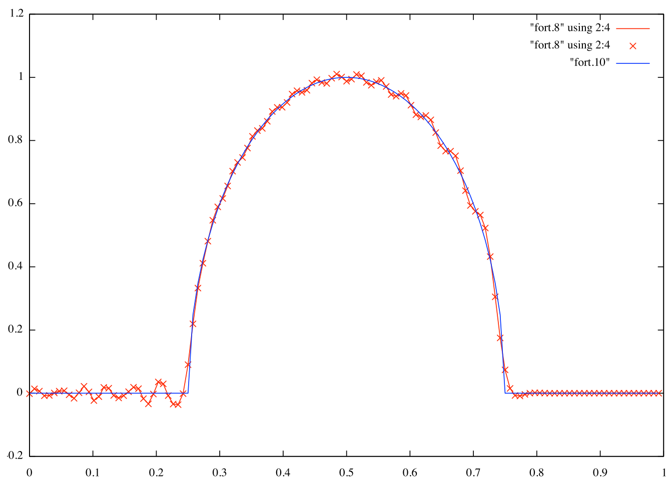

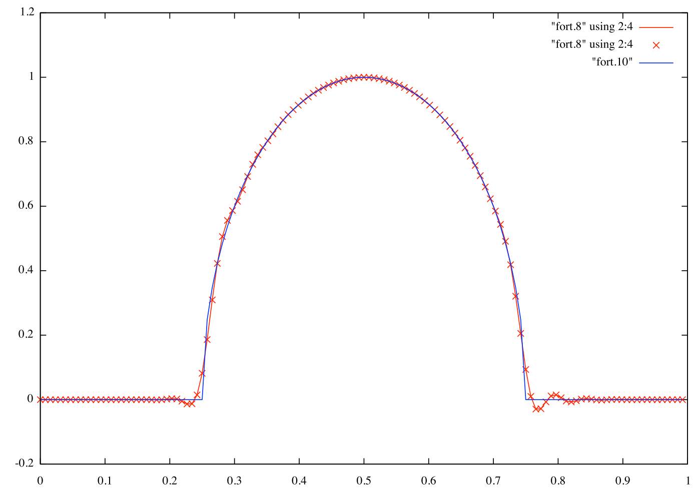

limiter

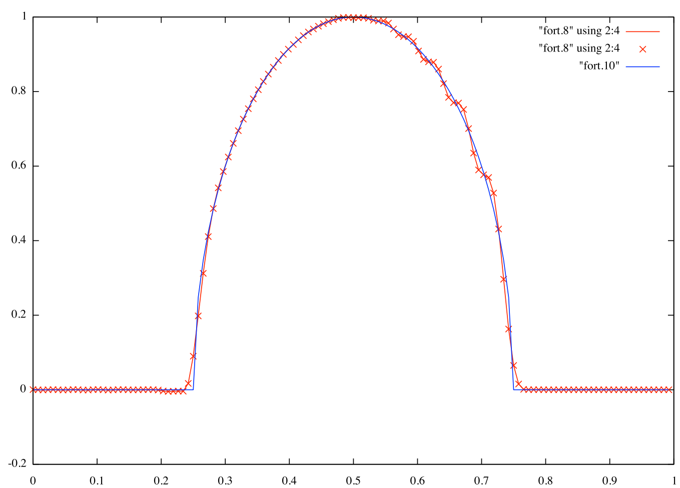

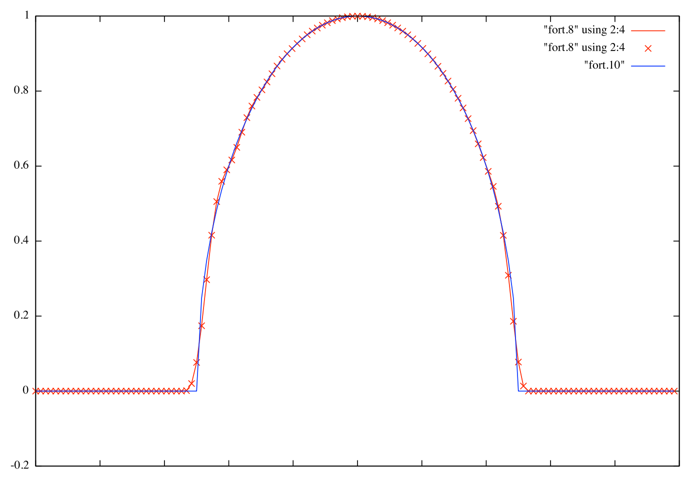

Convergence for sin^10 Initial Data (with limiter)

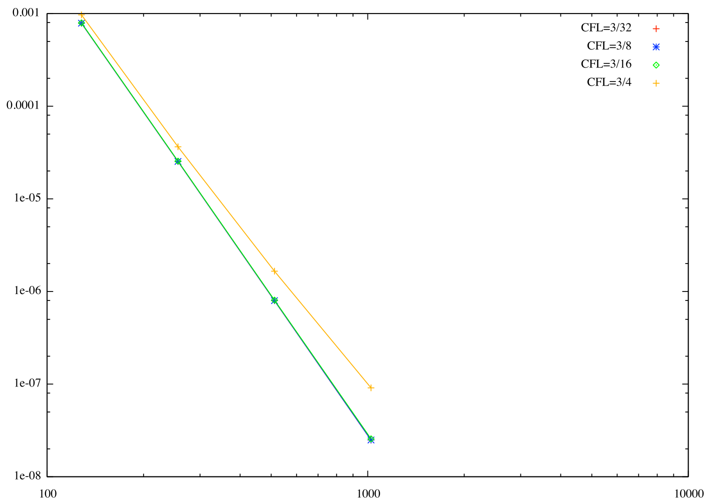

5th order in space

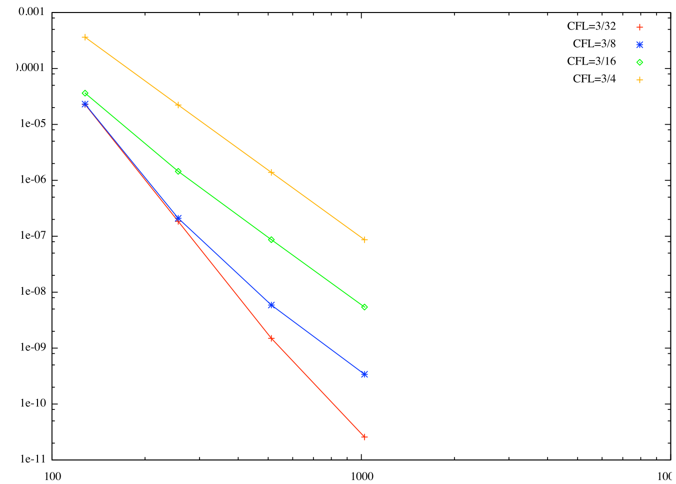

7th order in space

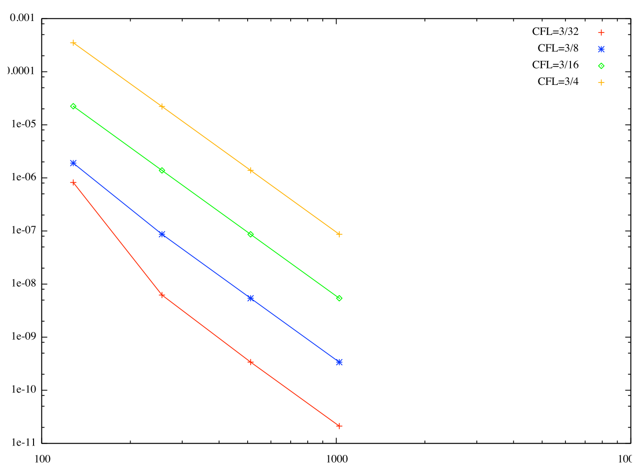

9th order in space

BERKELEY LAB
LAWRENCE BERKELEY NATIONAL LABORATORY

U.S. DEPARTMENT OF ENERGY | Office of Science

Square wave initial data
(n=128, T=10, with Limiter)

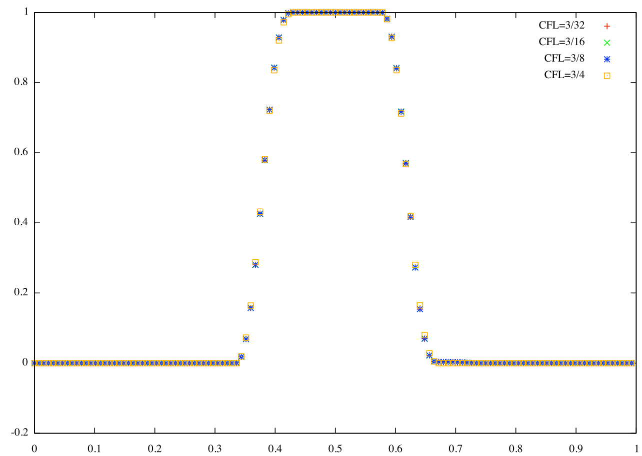

5th order in space

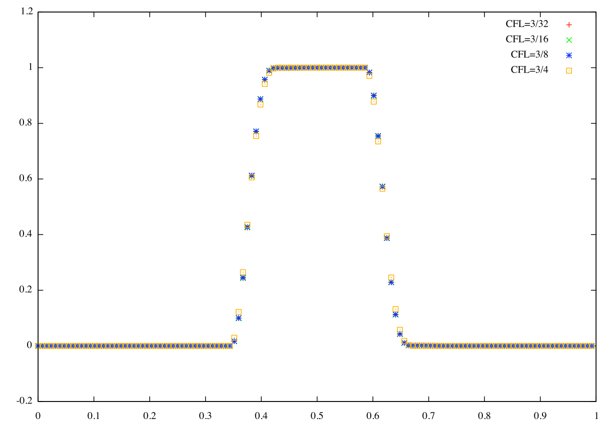

6th order in space (centered)

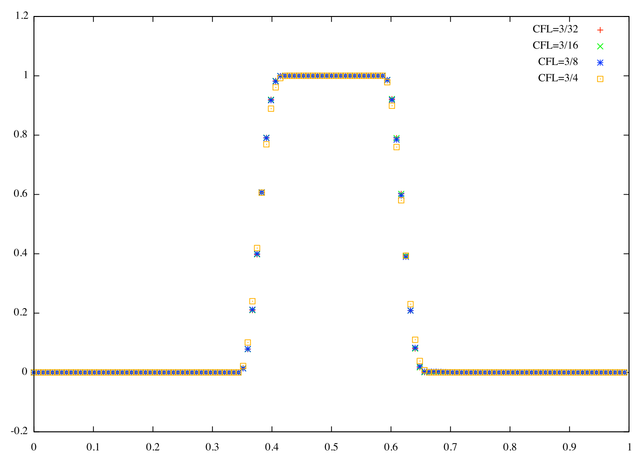

7th order in space

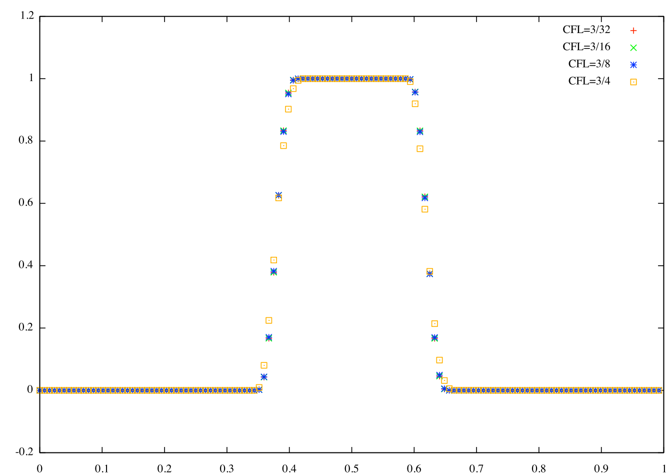

9th order in space

BERKELEY LAB
LAWRENCE BERKELEY NATIONAL LABORATORY

U.S. DEPARTMENT OF ENERGY | Office of Science

At High Order, Details Matter

At extrema:

- If sign of second derivative changes, use low-order fluxes (Colella and Sekora, 2008)
- If antidiffusive fluxes not antidiffusive, set them to zero (Zalesak 1979).

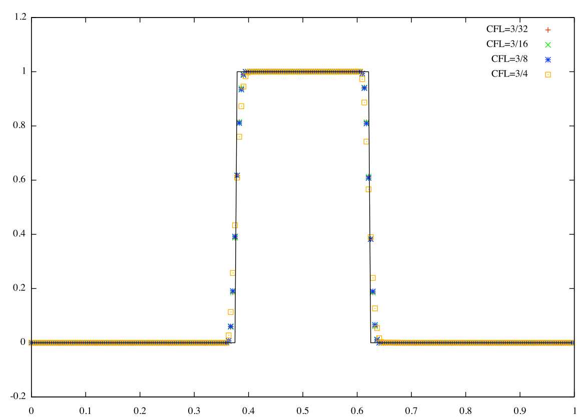

9th order in space

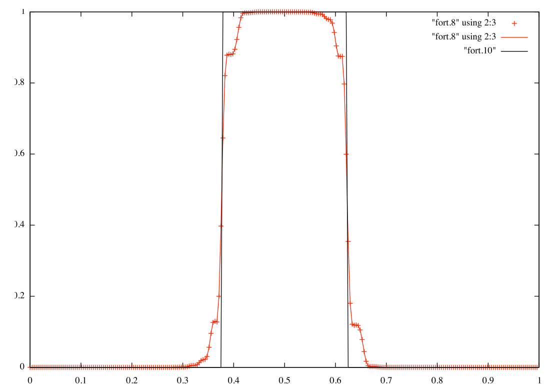

no Zalesak fix

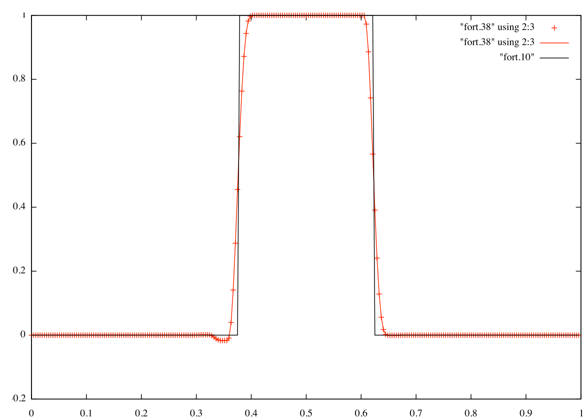

no CS fix

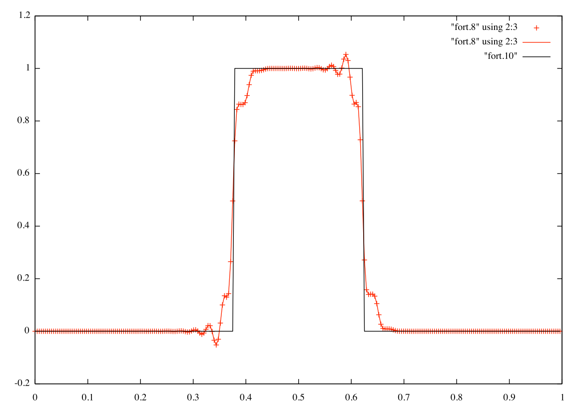

neither fix

BERKELEY LAB
LAWRENCE BERKELEY NATIONAL LABORATORY

U.S. DEPARTMENT OF ENERGY | Office of Science

Dimensions > 1

In higher dimensions, new considerations enter.

$$a(x, y) = x^3 - xy^2$$

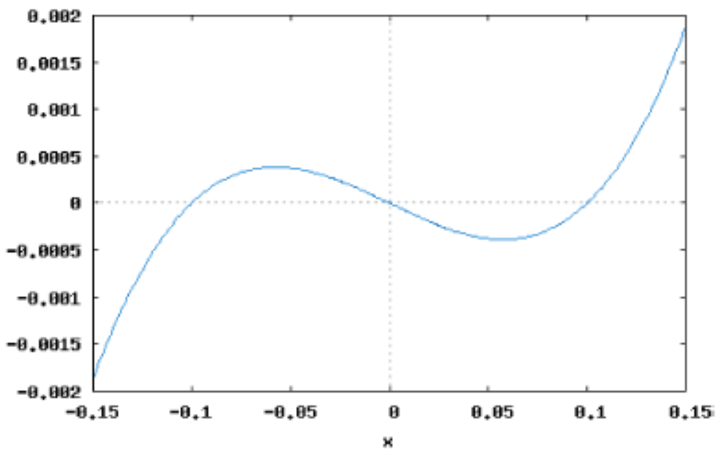

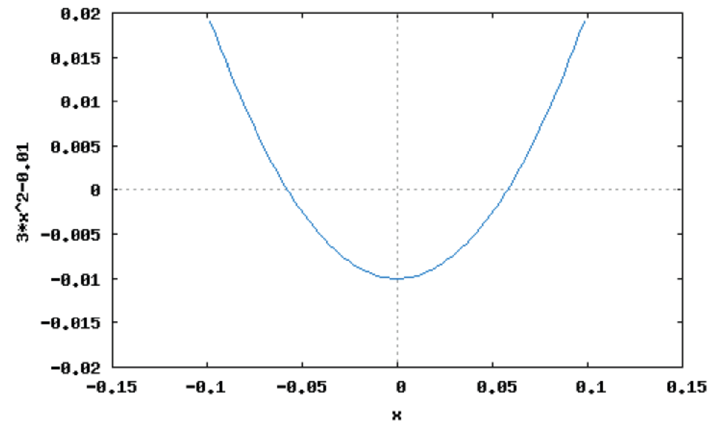

By choosing y sufficiently small, we can make the relative cell-to-cell change in D^2a as large as we want, turning on the limiter. This ends up polluting the solution accuracy more globally. An additional test to detect near-cubics is used to decide whether to apply a limiter.

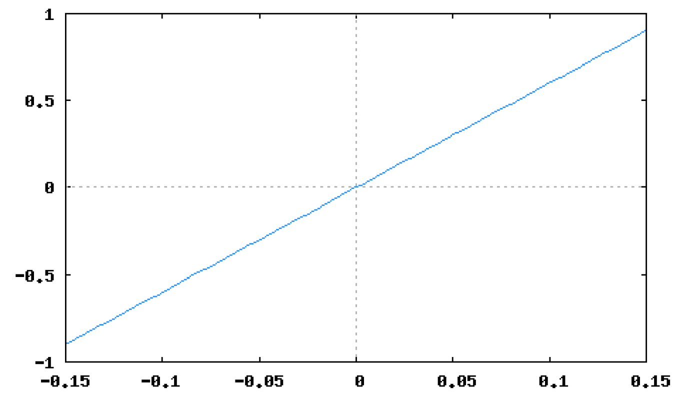

Conclusions and Future Work

Ongoing work:

• Extend upstream-centered method to multiple dimensions.

• Positivity preservation using redistribution.

• Ongoing applications development: incompressible Navier-Stokes, kinetic problems in plasmas, atmospheric modeling for climate, Maxwell's equations.

• Use of ARK methods for semi-implicit treatment of stiff terms.

• Extension of cut-cell methods to higher order.

Final comments:

• Basic framework for designing methods for discontinuous solutions to hyperbolic conservation laws developed in the late 1970's - early 1980's remains applicable to new settings, new requirements.

• AMR with spatial and temporal accuracy independently tunable might be much trickier, particularly for next-generation architectures.